THERMOSPRING: Thermal Exchange Reduction Mechanism using Optimized SPRING

California State Polytechnic University, Pomona

Caroline Herrera (Mechanical Engineering, Undergraduate)
Charles Johnson (Mechanical Engineering, Undergraduate)
Dominique Munoz (Mechanical Engineering, Undergraduate)
Osheen Gupta (Mechanical Engineering, Undergraduate)
Nathaniel Antonio (Mechanical Engineering, Undergraduate)

Advisor: Dr. Frank Chandler, PE.
Associate Professor, Aerospace Engineering Department
California State Polytechnic University, Pomona, CA

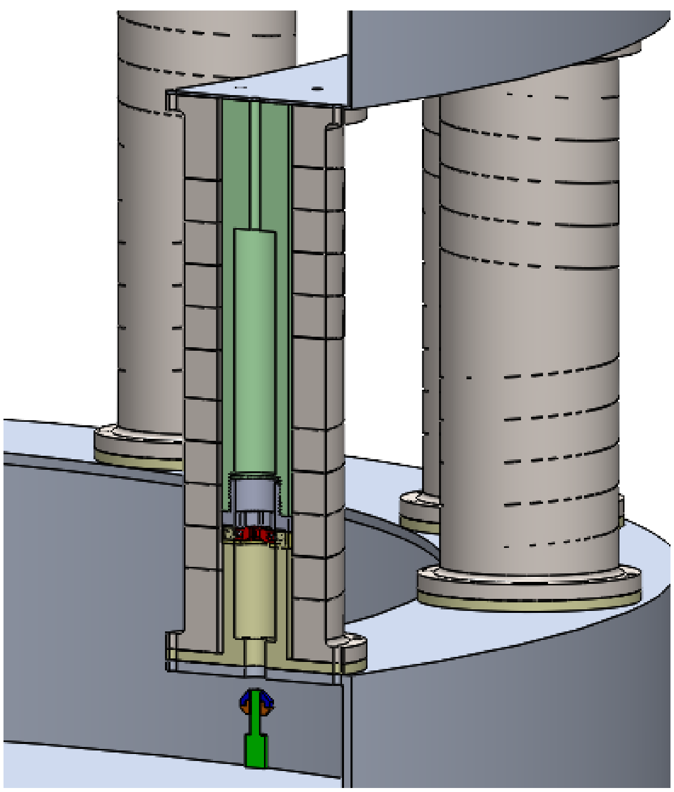

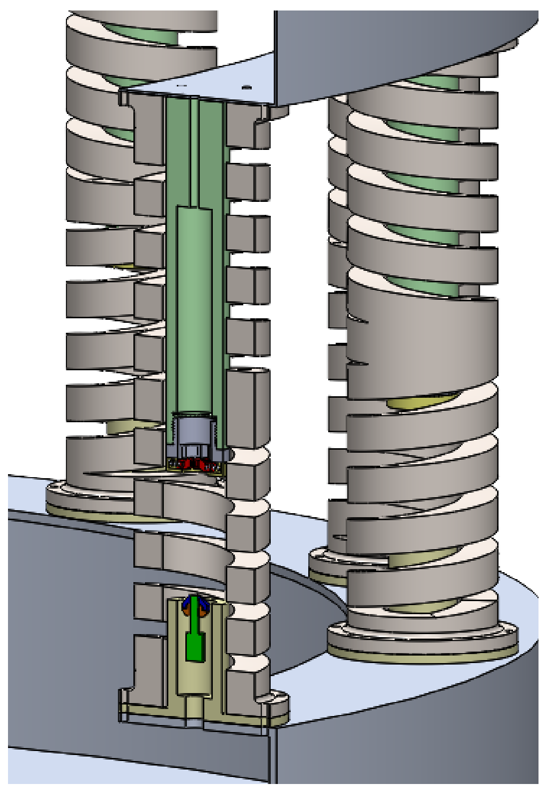

THERMOSPRING: Thermal Exchange Reduction Mechanism using Optimized SPRING

California State Polytechnic University, Pomona

Theme Category, Major Objectives & Technical Approach

- Theme Category: Advanced Structural Supports
- Major Objectives
  - Minimize heat transfer into the cryogenics tanks by innovative fully mechanical structural supports
- Technical Approach
  - Features a spring as a support due to springs being naturally better at thermally isolating components due to the long path heat has to travel through
  - Expansion and compression of springs based on gravity

Spring on earth

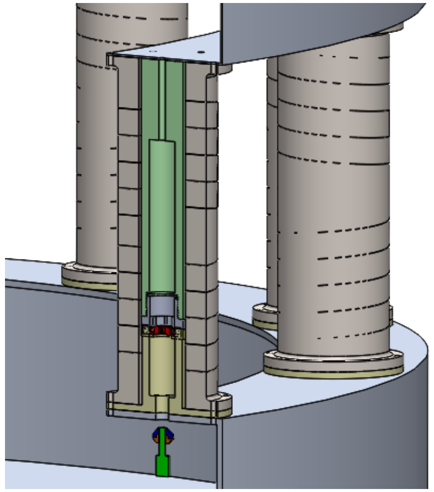

Spring in Orbit and on the Moon

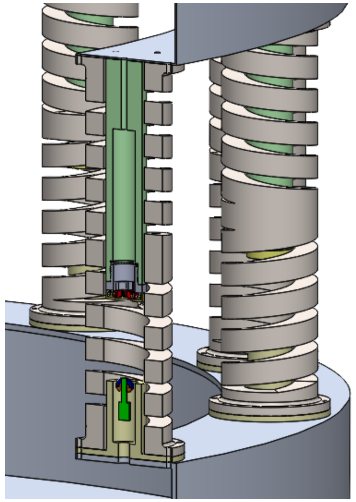

Key Design Details & Innovations of the Concept

Key Design

•Machined spring to reduce squirm, incorporate structural mounting, and improve manufacturability.

•Push-push lock to allow control of the system and eliminate premature expansion.

•Central columns are the main load-bearing path, allowing springs to be optimized for low g environments and thermal properties.

Innovations

•Upon researching, it appears that there is currently no design out there using springs as structural supports, hence our innovative design.

•Push-Push Lock allows for positive control over when the spring is allowed to extend.

•Using gravity to control expansion and reduce heat transfer eliminates many electrical components and costs.

Summary of Schedule & Costs for the proposed solution's path to adoption

- 3 year phased schedule to complete design, prototyping, testing, and full integration of THERMOSPRING, with Year 1 focusing on CAD and FEA, Year 2 on environmental testing and iteration, and Year 3 on flight hardware integration and launch readiness
- Joint efforts by design, analysis, and testing sub-teams to reduce project length
- $150k estimated budget, including $118K for materials and fabrication, with remaining funds allocated to testing, simulation tools, and integration

Table of Contents

Table of Figures

1. Introduction

1.1 Executive Summary

THERMOSPRING (Thermal Exchange Reduction Mechanism using Optimized SPRING) is an innovative structural support system using springs. It is designed to enhance cryogenic storage lifespan in space applications. Addressing the challenge of Advanced Structural Supports, this solution utilizes a spring-based system with concentric inner cylinders to minimize heat transfer.

Springs naturally provide superior thermal isolation compared to traditional hollow cylinders due to the long conduction path through the wire, significantly improving thermal resistance. The springs expand in space, separating the inner cylinders and eliminating conductive heat transfer through the inner cylinders. Beyond thermal benefits, the cylinders ensure structural stability during launch by preventing lateral movement in high-gravity environments. In addition to the cylinders, there is a mechanism called the "push-push lock" that keeps the spring compressed and locked to mitigate premature spring expansion and provide additional stability for the system in high gravity environments such as launch.

1.2 Specific Cryogenic Challenge

The chosen challenge was related to advanced structural supports that can minimize heat transfer into cryogenic tanks.

2. Solution

2.1 Overall Summary

The proposed solution features a spring system composed of 14 springs, each containing two concentric cylinders housed within the inner diameter of the spring. The inner cylinders have low thermal conductivity coating surrounding them. Springs are naturally better at thermally isolating components that need to be kept at a specific temperature due to the long distance (the coiled wire) that heat is forced to travel through. Springs are known to be several times more thermally isolating than hollow cylinders of both the same length as a compressed spring and the same thickness as the diameter of the springs' wire. In this case, our comparison led to a thermal resistance of the spring of $R = K/W$ compared to the typical flange-to-flange support of $R = K/W$. The difference is significant.

On Earth, components naturally weigh more due to Earth's gravity of $9.81\frac{m}{s^2}$ as opposed to the Moon's force of gravity at $1.625\frac{m}{s^2}$. This was used to our advantage in the development of THERMOSPRING, allowing us to make the invention nearly fully mechanical. The calculated weight of the structure and tank of liquid oxygen (LOX) on Earth was 6.1094e+06 kg and on the Moon was 9.6234e+05 kg. Due to the weight difference of the human landing system being deployed from Earth to the Moon, the compression spring will expand automatically once it is in space, in low gravity environments.

$$F = k\Delta x \rightarrow \Delta x = \frac{F}{k} \quad \text{where } \Delta x = \text{spring displacement}, F = \text{weight, and } k = \text{spring constant}$$

The expansion of the springs is critical. As soon as the spring expands, the two inner cylinders [shown in green and yellow on the cover page CAD model] separate and eliminate heat transfer by conduction that was occurring in compressed state. Therefore, the only two remaining ways of heat being transferred are the path of the spring wire and radiation in space.

The springs are designed to support the loading on top of them for constant 3 g's of force. The inner cylinders were needed for structural support during launch, for forces that can reach up to 15 g's, and to stabilize the system during launch. The inner cylinders are designed to be the main load bearing components. The springs are designed only to provide enough force to separate the columns in orbit on the lunar surface. Springs can move side to side or squirm. The inner cylinders prevent the possibility of excessive squirming while in high gravity environments. The second system that helps with lateral movement is the Push-Push lock mechanism.

The Push-Push lock mechanism is designed to ensure the system remains locked during launch, therefore ceasing the possibility of premature expansion. A linear actuator can release the lock to let the springs extend and, therefore, provide a thermal break between the inner cylinders. The lock can also be extended to recapture the forward part of the system to retract it aft to provide stability in the system for orbital maneuvers. Aft is towards the rear of vehicle, forward is towards the front.
The images on the left depict the full assembly while the spring is compressed. The images on the right are zoomed in section views of the compressed spring on the top and of the expanded spring on the bottom in low gravity environments such as the moon.

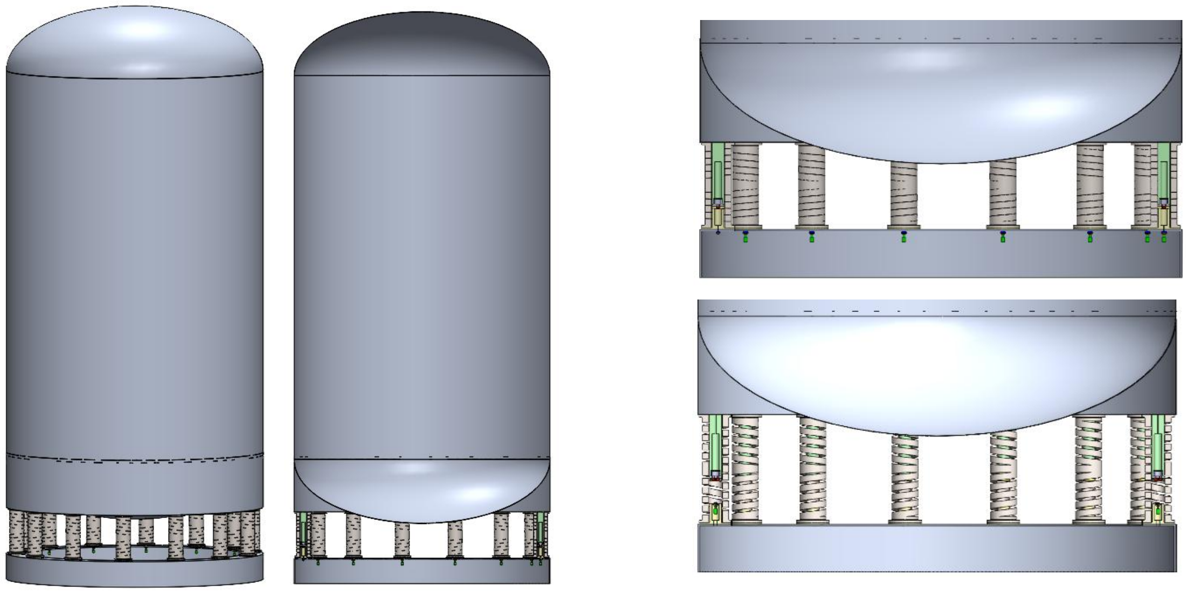

Figure 1: System Configuration and Cross sections

2.2 Changes Since the Proposal

There are two major changes that were made since the proposal: the spring shape from a circular cross section to a square wire and the addition of a push-push lock mechanism.

2.3 Constraints

This solution adheres to the minimal power requirement, poses no additional risks to crew on the human landing systems, can survive launch loads, has an operational life greater than the required several months, and is technology ready to be implemented on the moon within three to five years. Environmental calculations were made assuming the system is located on the south pole of the moon. More constraints and assumptions are indicated in their appropriate sections.

2.4 Materials

The materials for our system, operating in high stress during launch and microgravity environments in space, were chosen based on evaluation of strength-to-weight ratio, corrosion resistance, manufacturability, thermal characteristics, and cost-effectiveness. After comparing a multitude of potential material candidates, the team selected Ti-6Al-4V (Grade 5 Titanium) and 7075-T6 Aluminum with each component being optimized for its functional requirements for the THERMOSPRING and Push-Push lock mechanism.

Ti-6Al-4V was selected, having an exceptional combination of mechanical strength while having a relatively low density ($4.43\frac{g}{cm^3}$) compared to other metals. Along with having a very strong corrosion resistance, it maintains performance across a wide thermal range and demonstrates excellent fatigue behavior for high vibration conditions. This material was chosen for both the springs and pin for the

THERMOSPRING and the Push-Push lock mechanism, respectively. It also has aerospace documentation to back performance as listed in NASA's materials database [8], providing confidence in long term reliability and great compatibility with other spacecraft materials.

Aluminum 7075-T6 was chosen for the housing for the Push-Push lock mechanism. It offers one of the highest strengths to weight ratios among all aluminum alloys and is common among aerospace structural applications such as frames and fuselages. Additionally, aluminum is a readily available material making for high volume production and rapid prototyping [9], as well as the corrosion resistance being marginally higher than that of other aluminum grades.

2.5 Weight Assumptions

Tank Thickness Calculations: Thin wall approximation for pressure vessels was used to calculate the tank thickness for an assumed 40 PSI inner tank pressure for LOX. A thickness of 4mm was determined based on a 10m length, 5m diameter, 2:1 elliptical caps, and Aluminum 2219-T87 as the material.

Tank mass properties: A CAD model of the tank was created in SolidWorks. The empty tank mass was derived from SolidWorks' "Mass Properties," and the inner tank volume was calculated in the software as well. The inner tank volume was then used to calculate the mass of the LOX if the tank was theoretically full. The mass of the skirt was also retrieved from SolidWorks. With those three mass estimates, the total mass loaded onto the springs was calculated. Different total mass approximations were calculated depending on the amount of LOX left in the tank. The total weight on Earth was calculated using a 100 % LOX approximation. The total weight on the Moon was calculated using a 95% LOX approximation to account for boil off by the time the system reaches the Moon's surface. The 95% LOX on the Moon is only a starting point and decreases over time. A calculation with 0% LOX was used to figure out the maximum spring length when the LOX is fully utilized.

Skirt Thickness: Hand calculations were done to determine the approximate thickness that the skirt should be, and from there, there FEA was done in SolidWorks to determine if the thickness was suitable. A factor of safety (FOS) of 1.5 was used.

2.6 Spring Design

A machined spring was chosen over a traditional coil spring to improve manufacturing and material availability. This allows the spring geometry to incorporate a mounting flange and opposing twists to counter torsion in one unitary part.

The driving structural requirements were 14 springs, material Ti-6A1-4V, a FOS of 1.25, the maximum displacement of the springs (1 ft), an assumed 10 coils total, and a mean diameter of 0.21 m. The weight on Earth and the Moon was calculated. By using the change in force and max displacement, the spring constant, k, was calculated.

$$k_{spring} = \frac{\Delta F * FOS}{\Delta x_{max}}$$

$$b_{wire} = \left(\frac{k_{spring} * 44.5 * \mathrm{r}_{\mathrm{spring}}^{3} * \mathrm{n}_{\mathrm{coils}}}{G_{titanium}} \right)^{1/4}$$

where: b=square side length

The reason for a relatively short extension is to avoid structural issues for mechanisms on top of the cryogenic tank. Since the cryogenic tank system will be encased in a human landing system, it would be ideal to have the spring extension be minimal to prevent wasting space. The square side length of the wire was then calculated (0.0648 m side), along with other spring dimensions. Once initial calculations were completed, the total length of the spring on Earth and the Moon was found to be 0.6636m and 0.9074m, respectively. These lengths depended on the differing weights of the structure ab3ove the springs based on variation of gravity as well as the volume of cryogenic fuel left in the tank. The theoretical length of the springs when the LOX is completely utilized is 0.9528m.

2.7 Screw Selection

There are a total of 28 screws on this design that hold the concentric cylinders in place through expansion and compression. The screws were designed based on a FOS of 4.5 for amplified security; there was an inclusion of the launch loads that the system will be facing as well as the recommended FOS for design purposes. The material is steel with the specification of ASTM A574 with metric grade 12.9; minimum tensile strength of 1.17E9 Pa and minimum yield strength of 1.05E9. The screw is fine thread with a nominal size of 63.5mm, or 2 1/2 inches. The washer will be the same size as the screw with thickness of 6mm.

2.8 Push-Push Lock

A simple mechanism was designed to provide positive control over the spring system. A linear actuator extends through the central support column to insert the bayonet lug of the mechanism. Four paws retract as the jack screw extends. Once the first lug moves past the paws, the bayonet lug retracts to lock paws in place and compress the spring. To unlock, the jack screw extends until the decoupler moves past the locking paws. The jack screw then retracts as the spring reaches its free length under load, decoupling the support columns. Addition working procuring or designing a space rated jack screw is needed along with its drive motor.

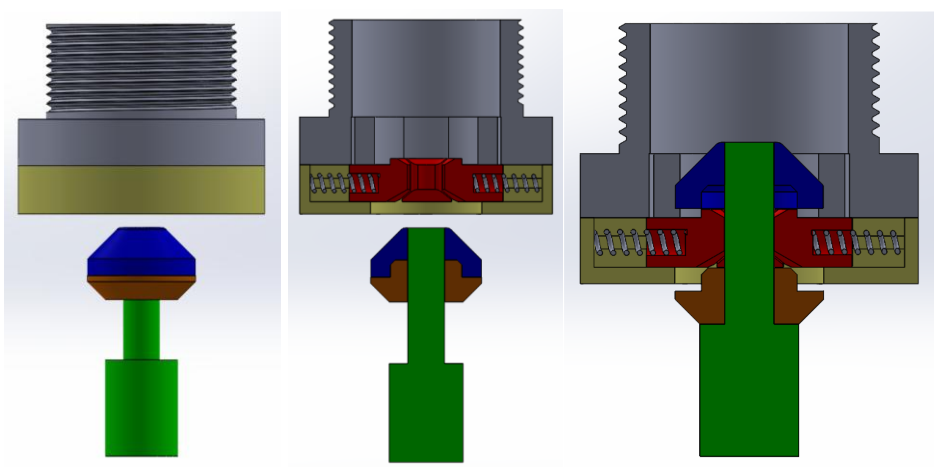

Figure 2: Push-Push Mechanism Configuration and Cross Sections

2.9 Solution Verification and Validation

2.9.1 Thermal Resistance Calculations

All lengths and areas were calculated from dimensions obtained from the CAD models. The values were then used to solve the thermal circuit for the THERMOSPRING in a typical flange-to-flange system. The calculated thermal resistance from the bottom of the flange to the top of the flange is simply the contact resistance between flange surfaces. The second thermal circuit was the spring in its compressed state in high gravity environments such as Earth. A third circuit was used for the expanded spring system in low gravity environments like orbit and the Moon. There were set temperature assumptions that were made to acquire the results displayed in Table 1. The top part of the flange is assumed to be the temperature of the LOX at 90 K. The bottom part of the flange is the temperature of the environment while on the moon at 166 K (calculated in Appendix A). These two assumed temperatures are used to calculate the heat flow through the springs. The solved thermal circuits are 1D heat flow from the bottom to the top of the springs using the pictures below.

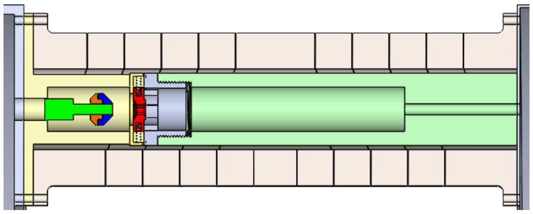

Figure 34: Spring Compressed

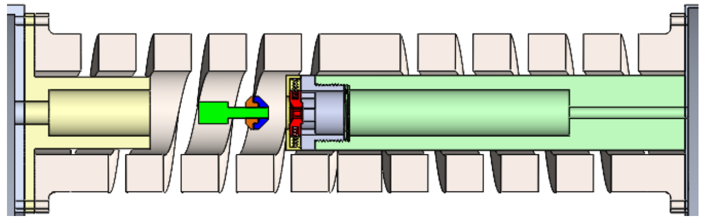

Figure 43: Spring Extended

The bowl area is where the cryogenic tank is integrated.

Table 1: Thermal Analysis Cases

CASE 1	**CASE 2**	**CASE 3**
Without THERMOSPRING	With compressed THERMOSPRING 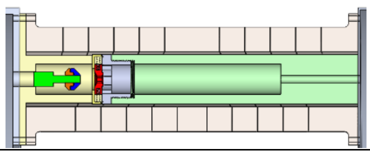	With expanded THERMOSPRING 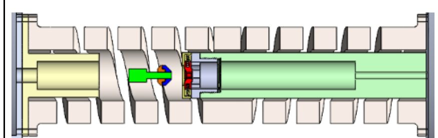
Flange to Flange	**Flange to Compressed Spring System to Flange**	**Flange to Expanded Spring System to Flange**
Applicable Environment This System Encounters: On Earth, in orbit, and on the moon	Applicable Environment This System Encounters: On Earth	Applicable Environment This System Encounters: In orbit, on the moon, or any low gravity situation.
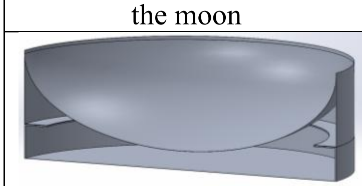	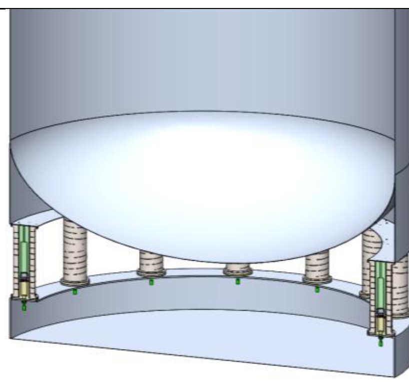	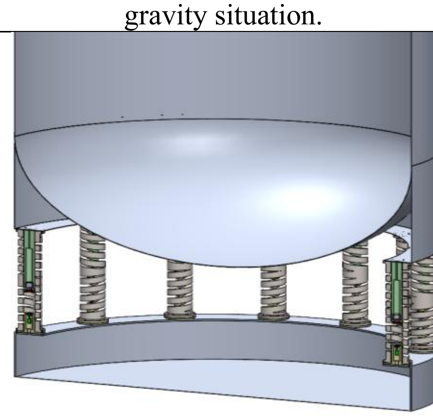
R_flange = 0.0396 K/W Q=1930 W	R_compressed = 1.5443 K/W q_compressed = 49.5189 W	R_expanded_spring = 16.75 K/W q_expanded_spring = 4.57 W

Table 22: Thermal Resistance and Heat Transfer Rate with and without THERMOSPRING

	Without THERMOSPRING		With THERMOSPRING	
	Rth (K/W)	Heat Rate Q=ΔT/Rth (W)	Rth (K/W)	Heat Rate Q=ΔT/Rth (W)
Pre-Launch (1-15 g, atmospheric)	R = 0.0396 K/W	Q=1930 W	R = 1.5443 K/W	Q = 49.5189 W
In Orbit (0 g, vacuum)	R = 0.0396 K/W	Q=1930 W	R = 16.75 K/W	Q= 4.57 W
On the Moon (0.17 g, vacuum)	R = 0.0396 K/W	Q=1930 W	R = 16.75 K/W	Q= 4.57 W

2.9.2 Thermal Analysis: Time to reach steady state

By assuming a lumped capacitance model, the time to reach steady state temperatures are calculated. Heat flow between nodes is $(T_j - T_i)/R$ from the thermal circuit with the LOX being a node at an initial temperature of 90 K, the bottom flange is at 166 K, and the spring is an average temperature of the LOX and the bottom part of the flange. The thermal circuit was used to derive the ODE's below and then a matrix was formed to solve for the time constants. Full calculations are shown in Appendix C.

$$\begin{cases} C_1 \dfrac{dT_1}{dt} = \dfrac{T_s - T_1}{R_1} \\ C_s \dfrac{dT_s}{dt} = \dfrac{T_1 - T_s}{R_1} + \dfrac{T_2 - T_s}{R_2} \\ C_2 \dfrac{dT_2}{dt} = \dfrac{T_s - T_2}{R_2} \end{cases} \rightarrow \frac{d\mathbf{T}}{dt} = A\mathbf{T}, \text{ with } A = \begin{bmatrix} -\dfrac{1}{R_1C_1} & \dfrac{1}{R_1C_1} & 0 \\ \dfrac{1}{R_1C_s} & -\dfrac{1}{R_1C_s} - \dfrac{1}{R_2C_s} & \dfrac{1}{R_2C_s} \\ 0 & \dfrac{1}{R_2C_2} & -\dfrac{1}{R_2C_2} \end{bmatrix}$$

$$\mathbf{T}(t) = e^{At}\mathbf{T}(0)$$

The following table gives a very rough ballpark number through hand calculations to show the effectiveness of the spring:

Table 3: Time-Constants for Case 1-3

	R (K/W)	τ=RC (s)	τ (h)	5τ (h) ≈99 % steady state
Case 1	0.0396	0.0396·1.07e5 ≈4.24e3	1.18 h	5.89 h
Case 2	1.5443	1.5443·1.07e5 ≈1.65e5	45.9 h	229.5 h (9.6 d)
Case 3	16.75	16.75·1.07e5 ≈1.79e6	497.8 h	2,489 h (103.7 d)

2.9.3 Thermal Desktop Analysis

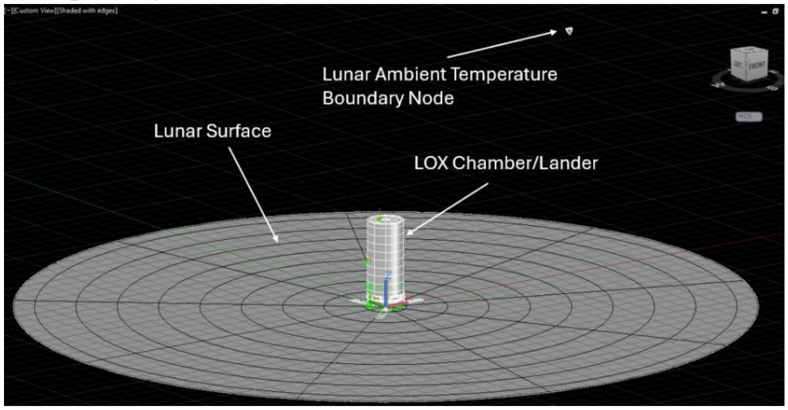

Figure 5: Lunar Surface Thermal Desktop Setup

A thermal model of a LOX storage chamber was developed to analyze heat transfer characteristics under lunar environmental conditions. The primary objective was to design a passive thermal control system that minimizes heat ingress into the LOX by implementing high thermal resistance pathways. The model includes thermal resistance calculations, ambient solar fluxes, and space temperatures, as well as the contact conductance through metal-metal interfaces. The Lunar Ambient Temperature boundary node accounts for the lunar surface mean temperature to ensure that the gradient across the regolith remains constant with what is expected.

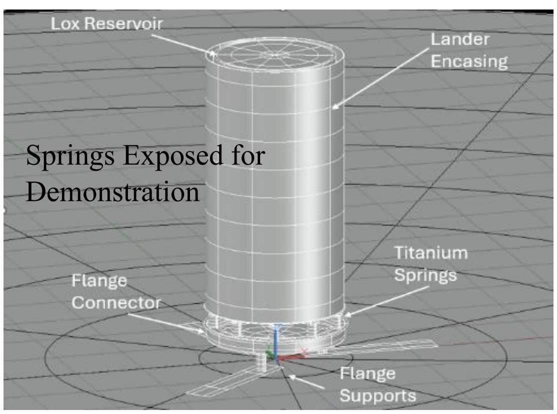

Figure 6: Thermal Desktop Tank Model

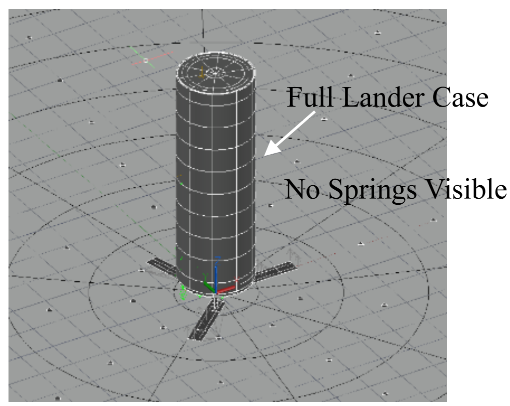

Figure 7: No Spring Radiation Model

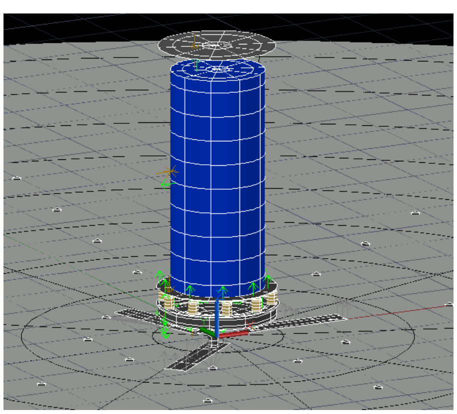

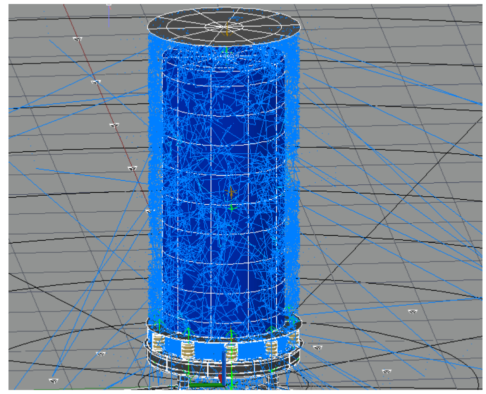

Figure 87: Radiation Thermal Conduction Model

Figure 9: Thermal Desktop Tank Model

The blue cylinder represents the LOX tank, and the beige columns at bottom represent the springs attached to the flange. The spring resistances were modeled through rigid bodies using the thermal resistance equation and solving a conductivity value to predict the temperature profiles of the springs. In flight, the LOX would be encased in a reservoir which would be encased by the HuLC lander. The blue lines in the figures above represent the radiation conductors that are reflecting through the system until a threshold minimum value of thermal energy is reached where the thermal energy transfer by radiation is negligible. The heating rate used is from solar flux for objects located around the south pole of the moon, using the orbit feature in thermal desktop

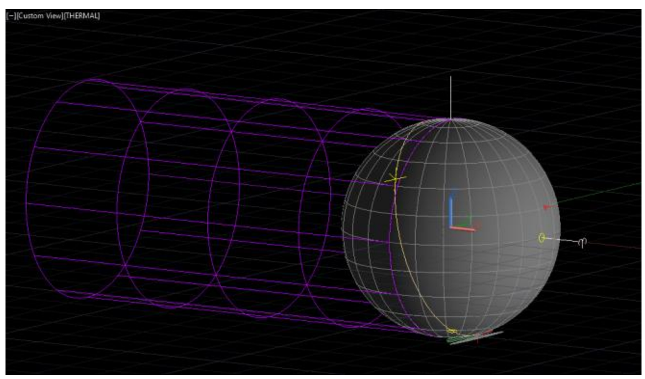

Figure 98: Thermal Desktop Orbit Model

The orbit is set to be controlled and constant around the bottom of section; this keeps it in a constant position on the moon as the moon orbits the earth and receives the estimated solar flux based on the incident light.

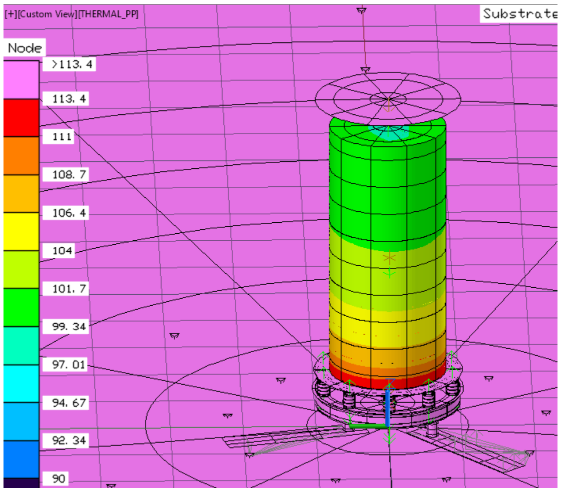

Figure 109: No Spring Thermal Resistance

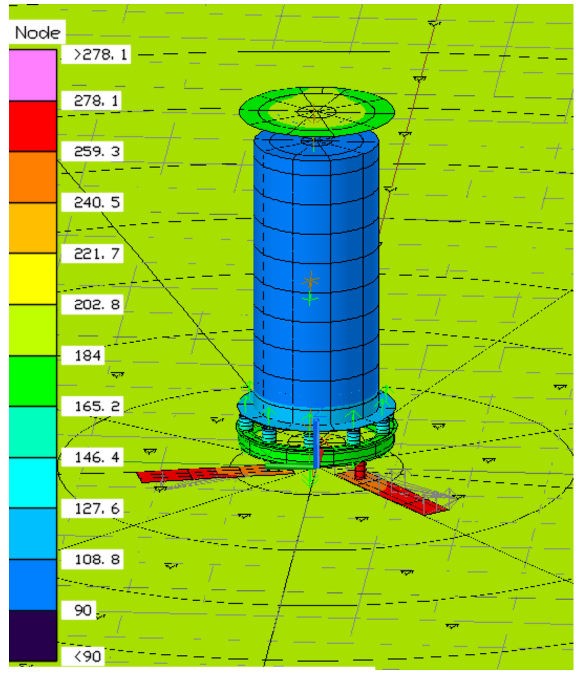

Figure 1110:Spring Thermal Resistance

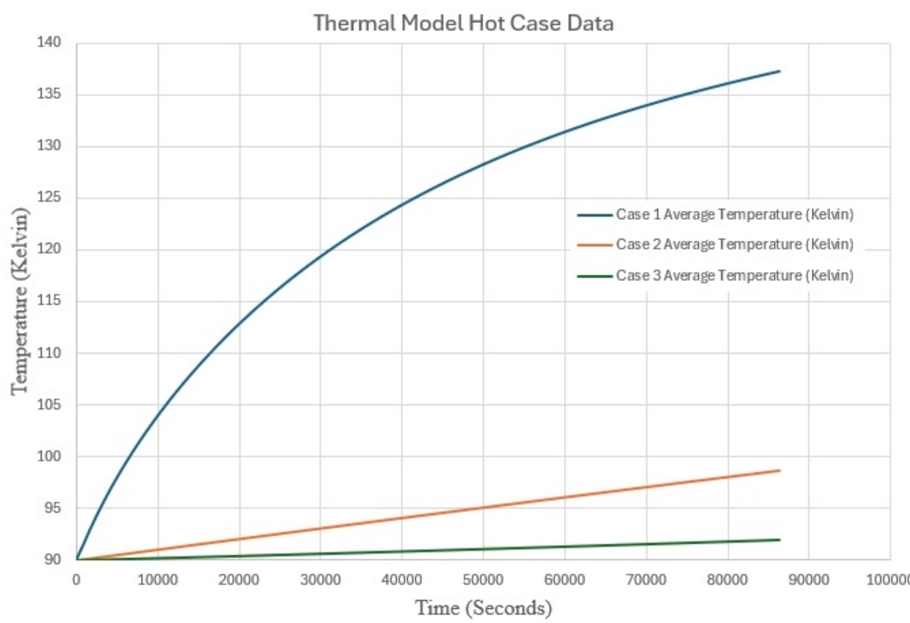

Figure 11: LOX Average Temperature

Final thermal performance was plotted in a transient simulation for all three cases with a simulation time of 86400 s (24 hours). Temperature profiles of every node were taken and averaged for this plot to show the benefit of the two different THERMOSPRING configurations versus without the THERMOSPRING. Starting from an initial temperature of 90 K for three different thermal resistances: In Case 1, with a very low resistance of 0.0396 K/W, the node warms rapidly toward its high equilibrium temperature of ≈137 K, achieving over 95 % of that rise in roughly 3.5 hours. Case 2, at a moderate resistance of 1.5443 K/W, exhibits a slower response and the temperature has climbed only to about 98 K. Finally, Case 3's high resistance of 16.75 K/W produces a very sluggish rise—so that even after 24 hrs the node temperature has barely increased above 90 K, approaching only ≈92 K. These results clearly illustrate how increasing thermal resistance both reduces the steady-state heat flow (and thus the final temperature rise) and lengthens the time required to reach thermal equilibrium. Raw temperature data for all the LOX nodes used in the thermal desktop model can be found in the appendix.

2.9.4 Obstacles with Development and Mitigation Strategies

Machined springs will require more testing as spring design equations provide only a starting point. testing will provide the information needed to geometrically optimize the spring. In addition, a space environment rated jack screw or linear actuator will need to be developed or procured to provide positive control over the system. Thermal analysis will also need to be validated through testing as well. Due to the ability for the tank and support to move, the system may require the use of bellows to allow fluid flow in its different configurations. Also, any cabling must be able to account for the expansion of the spring system as well.

3. Implementation

3.1 NASA Technology Readiness Level

The proposed system operates using mechanical principles and relies on a spring-based mechanism for functionality. An almost purely mechanical system reduces complexity as well as increasing its reliability. This ensures the system is robust in extreme environments, such as those encountered in aerospace applications.

Mechanical systems, such as those that include springs, are very common in aerospace applications, including vibration isolation and energy absorption systems. Passive mechanisms such as this one require very minimal maintenance and have predictable performance characteristics under varying loads and environmental conditions.

In terms of NASA's Technology Readiness Levels, the system aligns with TRL 2 and 3. The components (springs, structural components, fasteners) are prevalent in many similar passive mechanical systems that have been tested in both terrestrial and microgravity conditions. This approach guarantees a high degree of reliability along with aligning NASA's preference for proven, low-risk solutions in mission-critical applications.

3.2 Path-to-Flight Project Timeline

- **Year 1: Development Phase**
  - Q1-Q2: Requirements and Design
    - **Mission Requirements & Restraints**: Defining mission objectives, potential environmental constraints (temperature, radiation, pressure), and performance criteria that the THERMOSPRING must achieve. Accounting for extreme temperature fluctuations and material durability in a vacuum to scale for lunar applications.
    - **CAD Model:** Modeling and Designing a CAD model of THERMOSPRING with all key components, opening the door for simulations to optimize design before scaling the project.
    - **Material Trade Study & Selection:** Conducting research on materials that will be capable of withstanding the lunar environment such as high strength alloys or composites with low thermal conductivity. Along with materials that will provide a lightweight design as well as an easy manufacturing process.
    - **Coupon and Material Testing:** Material testing from prospective manufacturers to validate material properties and thermal conductance.
    - **Finite Element Analysis (FEA):** Conducting simulations on different parts of the THERMOSPRING to evaluate structural integrity, thermal response, and material stress. Will help visualize potential weak points prior to manufacturing.

- Q3-Q4: Refinement & Prototype Prep
  - **Design Iteration**: Based on FEA simulations and tests, make any necessary changes to the design.
  - **Manufacturing Readiness Plan:** Begin developing a plan to manufacture such as timeline, material sourcing, and fabrication methods. The plan should allow for scaling from prototype design to full scale production.
  - **Static Testing:** Conducting static tests to simulate structural response of material under expected loads during both landing and operation. Can scale conditions as needed to configure parameters appropriately.
  - **Build engineering design unit:** Once individual components have passed preliminary analysis, assembly tests can be performed to ensure functionality of the entire system under operating conditions.
  - **Functional Test:** Perform tests to ensure systems functions as intended.
- **Year 2: Testing & Refinement**
  - Q1-Q2: Durability & Thermal Testing
    - **Durability and Damage Tolerance Testing**: Long-term stability testing under fatigue conditions.
    - **Vibration Testing:** Simulating launch conditions to see vibrational reactions and operating stresses under shaker tables or other vibration generating equipment. Testing under high vibration frequencies will provide much needed insight into how THERMOSPRING will perform during launch.
  - Q3-Q4: Thermal Testing
    - **Thermal Cycling:** Exposing the prototype to different thermal extremes to simulate the lunar surface ranging anywhere from -200℃ to +120℃. This would allow assessment of the material's thermal expansion and expected behavior under lunar conditions.
    - **Design Iteration**: Based on testing results, any weaknesses discovered should lead to immediate revision of the prototype to better meet mission goals.
- **Year 3: Final Fabrication & Launch Preparation**
  - Q1-Q3: Flight Part Fabrication
    - **Flight Hardware Fabrication:** Begin fabrication of components of THERMOSPRING using selected materials and manufacturing methods identified in Year 1.
    - **System Assembly & Integration:** The THERMOSPRING system will begin to be fully assembled and integrated. Full integration testing will be conducted at the same time.
  - Q4: Testing
    - **Final Testing:** Performing a set of acceptance tests to ensure all mission criteria has been met, such as functionality, quality assurance, and final safety assessments. This phase will verify the system's ability to withstand launch and landing conditions.
    - **Flight Certification & Path to Adoption:** Submit for mission integration, demonstrating TRL 2-3, and finalizing all documentation for path to flight endorsement

3.3 Budget Assessment

A detailed budget assessment is provided in this section, which covers labor expenses and material costs, along with a comprehensive cost margin analysis. This is based on realistic estimates, as well as the use of analogs and NASA's costing tools. The primary goal is to ensure that the projected budget stays in line with NASA's standards for development and integration of the system. The total costs of the system as mentioned includes materials, labor, and manufacturing costs. The estimated costs shown below are derived from analysis of similar systems as well as considering industry standard estimates:

Table 34: Cost estimations

Component	Quantity	Unit Cost ($)	Labor (Hrs)	Total ($)
Spring	14	3,471.16	4,000	80,596.24
Outer Cylinder	1	376.32	8	1016.32
Inner Cylinder	1	35.31	8	675.51
Skirt	1	1530.84	4,000	33,530.84
Screws	28	100	0	2,800
Washers	28	5	0	140
Push-Push Lock	14	1038.43	8	14,538.02
Total	-------------	-----------	------------	133,297
Budget	-------------	-----------	-----------	150,000

Labor Assumptions: $80/hr (this is based on the time needed for assembly and integration of the system).

Cost Margin and Markup Evaluation

Included in the calculation for total cost is overhead, reliability, and other financial considerations. The following calculation shows the markup:

Cost Margin
150,000(3) = 450,000
450,000-150,000 = 300.000
300,000/450,000 = 0.667
0.667(100) = 67% markup rate

This markup percentage is intended to cover indirect costs like overhead and profit margin. Which aligns with the industry norm's financial structure, ensuring a balanced budget for development and production.

Use of Analogs and NASA Costing Tools

To ensure validation of the cost estimate, we referred to NASA's HuLC resources, which provided a benchmark for similar systems. Such analogs provided valuable insight into cost structures for comparable projects; this allowed us to make informative decisions about material selection, labor, and integration costs. Additionally, NASA's costing tools were used to model the expected expenses in this process of developing and integrating such a system, making sure the budget is accounted for in all relevant stages of this project.

System Development and Operation Considerations

Although the technology that is used in this project is mostly mechanical, which keeps simplicity, the project's system development and operational phases are critical to the mission's success. The following considerations have been factored into the budget:

- System Development: Assembly and integration of all components, as well as testing and verifying that the system functions completely.
- Mission Infusion: Once fully developed, the system will be adopted for operational use. Costs associated with the infusion into mission operations have been included, with a precise focus on efficiency and long-term reliability.

- Integration: Labor costs associated with integrating components into the system, such as final testing, have all been incorporated into the total budget which ensures all parts function together seamlessly.
- Operations: Maintenance, monitoring, operational costs, or any updates during the system's lifespan, are included in the overall budget to ensure ongoing mission success.

The projected budget for the system has been assessed thoroughly, utilizing NASA's costing tools and analogs guarantees accuracy. The total estimated budget of $150,000 includes all labor and material costs, along with a cost margin to cover any overhead costs. This assessment aligns with NASA's expectations for system development, integration, and long-term sustainability.

4. Conclusion

The THERMOSPRING concept demonstrates a dramatic improvement in cryogenic thermal isolation by leveraging a mechanically actuated spring support that expands in low-gravity environments. From our thermal-circuit analysis (Table 1), the baseline flange-to-flange path exhibits a thermal resistance of only 0.0396 K/W (heat rate ≈1930 W). When the spring bank is compressed (earth gravity), the resistance rises to 1.544 K/W (≈49.5 W), and in the fully expanded configuration (orbit or lunar surface), it reaches 16.75 K/W (≈4.57 W). This corresponds to a 99.76 % reduction in parasitic heat flow compared to a rigid support. Mechanically, the Ti-6Al-4V inner-cylinder legs carry launch loads up to 15 g while the springs—sized for a constant 3 g preload—act as the sole elastic element in orbit, ensuring reliable deployment without additional power or active controls. A push-push lock maintains compression during ascent and releases automatically in microgravity, preserving structural stability and thermal performance.

With a nearly fully mechanical design, proven materials, a path to flight-ready TRL 2-3 within three years, and a total projected development cost under $150 k, the THERMOSPRING directly supports NASA's long-term lunar exploration goals, enabling longer mission durations and improving fuel efficiency for sustained operations on the Moon and beyond.

5. References

[1] NASA's Plan for Sustained Lunar Exploration and Development

[2] NASA's Initial and Sustained Artemis Human Landing Systems

[3] SLS-SPEC-159 NASA Cross-Program Design Specification for Natural Environments (DSNE) Revision I

[4] NASA Selects Blue Origin, Dynetics, SpaceX for Artemis Human Landers - NASA. (2020, April 30). https://www.nasa.gov/humans-in-space/nasa-selects-blue-origin-dynetics-spacex-for-artemis-human-landers/

[5] NASA Selects Five U.S. Companies to Mature Artemis Lander Concepts - NASA. (n.d.). https://www.nasa.gov/news-release/nasa-selects-five-u-s-companies-to-mature-artemis-lander-concepts/

[6] Beer, F. P., E Russell Johnston, Dewolf, J. T., & Mazurek, D. F. (2015). *Mechanics of materials* (8th ed.). Mcgraw-Hill Education.

[7] Design and Implementation of Thermal Control Strategy for Micro-size Lunar Exploration Rover HAKUTO - Scientific Figure on ResearchGate. Available from: https://www.researchgate.net/figure/External-and-internal-heat-flow-on-the-lunar-surface_fig1_335110388 [accessed 4 Mar 2025]

[8] NASA. *Titanium Alloy Ti-6Al-4V Properties*. NASA Materials Data Handbook. https://ntrs.nasa.gov/api/citations/19720022814/downloads/19720022814.pdf

[9] NASA. *Aluminum Alloy 7075-T6 Properties*. NASA Materials Data Handbook. https://ntrs.nasa.gov/api/citations/19670004550/downloads/19670004550.pdf

6. Appendices

APPENDIX A. Environmental Calculations

```
sigma=5.67*10^-8
T_LOX_C=-183 % Celsius
T_LOX_K=T_LOX_C+273.15 % Kelvin
T_infinity_C=54
T_infinity_C=T_infinity_C+273.15
emmissivity_lunar_surface=0.96 % lunar surface. page 276
solar_flux_mean=1367 %W/m2 pg 201
solar_irradiance=solar_flux_mean
albedo=0.12 %  (lunar near side)
reflectivity_mean=154 % W/m2
incidence_angle=86 %84-90 degrees from document
incidence_angle_radians=86*(pi/180)
k_surface_layer = 7.4*10^-4


% AZ-93 Coating for skirt/flange surfaces
emmissivity_surface=0.91
absorptivty_surface=0.15


% MLI Surface Info
emmissivity_MLI=0.05
absorptivty_MLI=0.12


% Temperatures
T_south_pole=(((1-
albedo)*solar_irradiance*cos(incidence_angle_radians))/(emmissivity_lunar_surface
* sigma))^(1/4) %pg 275-3.4.6.1 Lunar surface radiative environment
T_lunar_K=T_south_pole
T_lunar_C=T_lunar_K-273.15


T_skirt_C=T_lunar_C  % JUST AS ROUGH APPROXIMATION FOR NOW
T_skirt_K=T_skirt_C+273.15


T_space_K=3 % K. Space sink temp. From document
T_MLI_C=-100 % C
T_MLI_K=T_MLI_C+273.15


% Heat flow skirt
F_si=0.5 % radiation view factor sun to skirt surface
F_Li=0.5 % radiation view factor lunar surface to skirt surface
```

```
F_sp=0.5 % radiation view factor space to skirt surface
Ai=1/2*pi*D_skirt*L_skirt % Surface area of half of the curved area
Asp=Ai   % surface area view from space to the skirt. happens to be same as Ai
Q_sun=absorptivty_surface*F_si*Ai*solar_irradiance
Q_albedo=albedo*Q_sun
Q_surface=emmissivity_lunar_surface*emmissivity_surface*F_Li*Ai*sigma
Q_space=emmissivity_surface*Asp*F_sp*sigma*(T_skirt_K^4-T_space_K^4)
Q_total=Q_sun+Q_albedo+Q_surface-Q_space


% Heat flow tank
F_st=0.5 % radiation view factor sun to tank MLI surface
F_Lt=0.5 % radiation view factor lunar surface to tank MLI surface
F_spt=0.5 % radiation view factor space to tank MLI surface
Atank=1/2*pi*D_outer*L_outer % Surface area of half of the curved area
Asptank=Atank   % surface area view from space to the tank. happens to be same as
Ai
Q_sun_tank=absorptivty_MLI*F_st*Atank*solar_irradiance
Q_albedo_tank=albedo*Q_sun_tank
Q_surface_tank=emmissivity_lunar_surface*emmissivity_MLI*F_Li*Atank*sigma
Q_space_tank=emmissivity_MLI*Asptank*F_spt*sigma*(T_MLI_K^4-T_space_K^4)
Q_total_tank=Q_sun_tank+Q_albedo_tank+Q_surface_tank-Q_space_tank


T_env_eff_K = (F_Lt * T_lunar_K^4 + F_spt * T_space_K^4)^(1/4)
T_env_eff_C=T_env_eff_K-273.15
```

APPENDIX B. Thermal Circuit

Thermal circuit: all lengths and areas were calculated from getting dimensions from the CAD models. The values were used to solve the thermal circuit for the THERMOSPRING in its compressed state which would be while it is in high gravity environments and in this case Earth. A second thermal circuit was calculated to solve for a flange to flange system. A third circuit was calculated to solve for a flange to spring to flange system expended on the moon or any lower gravity environment.

```
L_12=0.01288
A_bolt_12=.001


L_23=.0046
A_washer_23=.00158
A_screw_23=.0031


L_34=.017
A_bottom_flange_34=5.266/N_spring
A_screw_34=A_screw_23
```

```
L_45=.07849
A_screw_45=A_screw_23
A_cylinder_45=.0041


L_56=.30151
A_cylinder_56=.00442


L_67=0.07960
A_outer_cyl_67=.00239 % CHECK
A_inner_cyl_67=.00203
A_coating_67=.00072


L_78=.09042
A_screw_78=A_screw_23
A_inner_cyl_78=.000993
A_outer_cyl_78=A_outer_cyl_67 %check
A_coating_78=A_coating_67


L_89=.005
A_flange_89=4.11658/N_spring
A_screw_89=A_screw_23


L_910=L_23
L_1011=L_12
A_screw_910=A_screw_23
A_washer_910=A_washer_23
A_bolt_1011=A_bolt_12


T_LOX_C=-183 % Celsius
T_LOX_K=T_LOX_C+273.15 % Kelvin
T_bottom_K=T_env_eff_K


K_t=K_titanium % titanium
K_al=120
K_coating=2
R12=L_12/(K_t*A_bolt_12)
R23=(1/(L_23/(K_t*A_washer_23))+1/(L_23/(K_t*A_screw_23)))^(-1)
R34=(1/(L_34/(K_al*A_bottom_flange_34))+1/(L_34/(K_t*A_screw_34)))^(-1)
R45=(1/(L_45/(K_t*A_cylinder_45))+1/(L_45/(K_t*A_screw_45))^(-1))
R56=L_56/(K_t*A_cylinder_56)
```

```
R67=(1/(L_67/(K_t*A_outer_cyl_67))+1/(L_67/(K_t*
A_inner_cyl_67))+1/(L_67/(K_coating* A_coating_67)))^(-1)
R78=(1/(L_78/(K_t*A_outer_cyl_78))+1/(L_78/(K_t*
A_inner_cyl_78))+1/(L_78/(K_t*A_screw_78))+1/(L_78/(K_coating* A_coating_67)))^(-
1)
R89=(1/(L_89/(K_t*A_flange_89))+1/(L_89/(K_t* A_screw_89)))^(-1)
R910=R23
R1011=L_1011/(K_t*A_bolt_1011)
Req_48=R45+R56+R67+R78
R_total_spring=(1/Req_48+1/(L_wire/(K_t*A_wire)))^(-1)
R_total_compressed1= R12+R23+R34+R_total_spring+R89+R910+R1011
R_total_compressed=R_total_compressed1/N_spring
q_total_compressed=(T_LOX_K-(T_bottom_K))/(R_total_compressed1/N_spring)


%R flange to flange
L_12f=L_12*2  %random screw tip length
A_screw_12f=A_screw_23


L_23f=L_12
A_nut_23=A_washer_23
A_screw_23f=A_screw_23


R12f= L_12f/(K_t*A_screw_12f)
R23f=(1/(L_23/(K_t*A_nut_23))+1/(L_23/(K_t*A_screw_23))^(-1))


R_total_flange_to_flange=R12f+R23f+R34+R89+R910+R1011


q_total_flange_to_flange=(T_LOX_K-(T_bottom_K))/(R_contact)
Rtot1=R34+R_total_spring+R89
Rtot2=R34+R89
diff=Rtot1-Rtot2


R671=(1/(L_67/(K_t*A_outer_cyl_67))+1/(L_67/(K_t* A_inner_cyl_67)))^(-1)
R781=(1/(L_78/(K_t*A_outer_cyl_78))+1/(L_78/(K_t*
A_inner_cyl_78))+1/(L_78/(K_t*A_screw_78)))^(-1)


Acyl=pi/4*OD^2-pi/4*ID^2
Rcyl=L_earth/(K_t*Acyl)
R_expanded_spring_wire=(L_wire/(K_t*A_wire))/N_spring
q_expanded_spring_wire=(T_LOX_K-(T_bottom_K))/(R_expanded_spring_wire)
R_cyl_solid=L_earth/(K_t*pi*(OD/2)^2) %if solid cyl only
```

Fastener Calculation [Imperial]:

APPENDIX C. Steady-State

```
m1     = 1.9493e5;     % kg (top mass)
cp1    = 1400;         % J/(kg·K) (top mass)
ms     = 2.9257e3;     % kg (spring mass)
cps    = 526.3;        % J/(kg·K) (spring mass)
m2     = 783;          % kg (bottom mass)
cp2    = 864;          % J/(kg·K) (bottom mass)
R_spring = 16.75;    % K/W (total spring thermal resistance)
R1 = R_spring/2;       % split equally top-spring
R2 = R1;               % and spring-bottom
C1 = m1*cp1;
Cs = ms*cps;
C2 = m2*cp2;
A = [ ...
   -1/(R1*C1),         1/(R1*C1),          0;
    1/(R1*Cs),   - (1/(R1*Cs)+1/(R2*Cs)),  1/(R2*Cs);
    0,                  1/(R2*C2),    -1/(R2*C2) ...
];
% Initial conditions (K)
T1_0 =  90;                     % initial top-mass temperature
T2_0 = 166;                     % initial bottom-mass temperature
Ts_0 = (T1_0 + T2_0)/2;        % initial spring temperature
T0   = [T1_0; Ts_0; T2_0];
% Time
eigVals = eig(A);
timeConstants = -1./eigVals;    % seconds
t_final = 5 * max(timeConstants(~isinf(timeConstants)))
tspan = [0, t_final];
t_final_hours = t_final/3600
t_final_days=t_final_hours/24
```

APPENDIX D. Bolt Selection

Material	Min Tensile Strength (psi)	Min. Yield Strength (psi)	Proof Strength (psi)	Preload Strength (psi)
ASTM A574 Socket Head Cap Screw (over 1/2 - 4 in)	170000	153000	135000	101250

Nominal Size Bolt Dia(in)	Thread	Head Width (in)	Head Height (in)	Tpi	Tensile Stress Area (in^2)	Nominal Stress Area (in^2)
2 1/2	Fine	3 3/4	1 5/8	12	4.6000	4.5951

Nominal Size Nut (in)	Nut Width (in)	Nut Height (in)
2 1/2	#N/A	#N/A

Nominal washer size (in)	Style	Inside Basic Dia (in)	Outside Basic Dia (in)	Basic Thickness (in)
2 1/2	USS	2.625	5	15/64

Torque (lb in)	Friction coe
232875	0.2

Joint Pressure (psi)	
31990.23978	
Width nut/head Hex (in)	
3 3/4	
Width nut/head Socket (in)	
3 3/4	

Number of Bolts	1
Bolt dia (in)	2 1/2
Preload (lbs)	465750
Width nut/head (in)	3 3/4
Internal Dia (in)	2.49
Internal Area (in^2)	4.870
Force Joint (lb)	32701
Force Bolt External (lb)	32701
Preload Min(lbs)	302738
Preload Max (lbs)	535613
Thickness Joint (in) (Total)	1.3855
Thickness Washers (in)	0.469
Grip Length (in)	1.854
k Washer (lb/in)	1.737E+08
k Joint Material (lb/in)	1.864E+08
k Total Joint (lb/in)	4.495E+07
k Bolt (lb/in)	2.369E+07
C	3.451E-01

Force Bolt Min (lb)	313801
Force Bolt Nom (lb)	476813
Force Bolt Max (lb)	546676
Yield FOS Min	1.98
Yield FOS Nom	1.30
Yield FOS Max	1.14
Load Factor Min	28.77
Load Factor Nom	14.03
Load Factor Max	7.72
Joint Sep Fos Min	13.99
Joint Sep Fos Nom	21.52
Joint Sep Fos Max	24.75

APPENDIX E. Raw Thermal Desktop Data

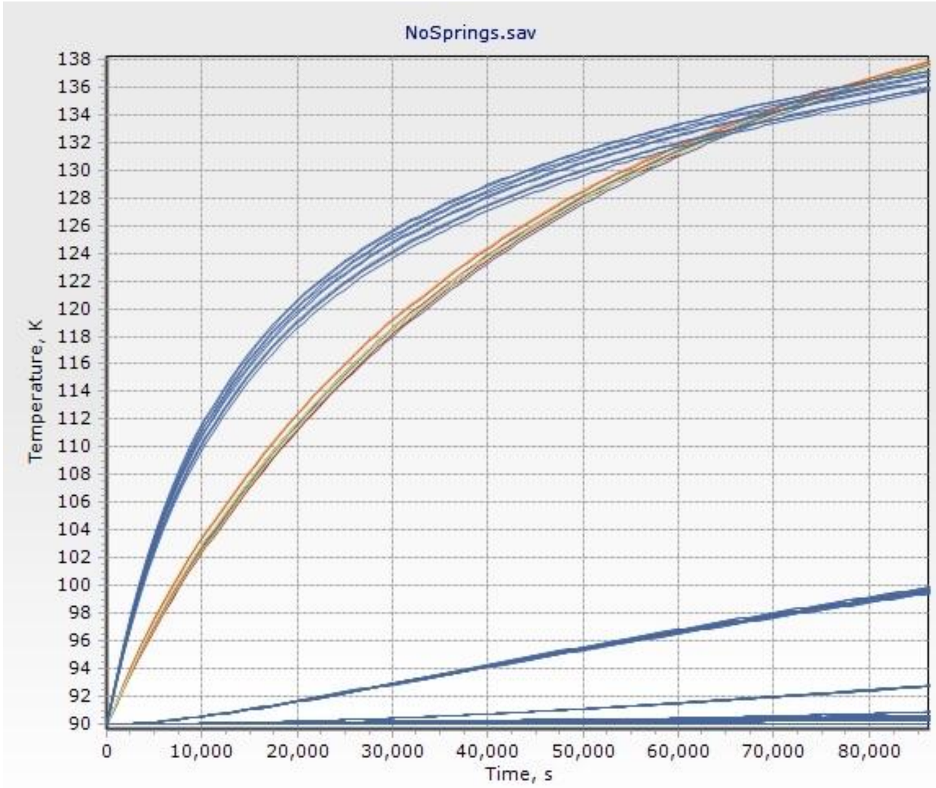
NoSprings.sav
Temperature, K
138
136
134
132
130
128
126
124
122
120
118
116
114
112
110
108
106
104
102
100
98
96
94
92
90
0
10,000
20,000
30,000
40,000
50,000
60,000
70,000
80,000
Time, s

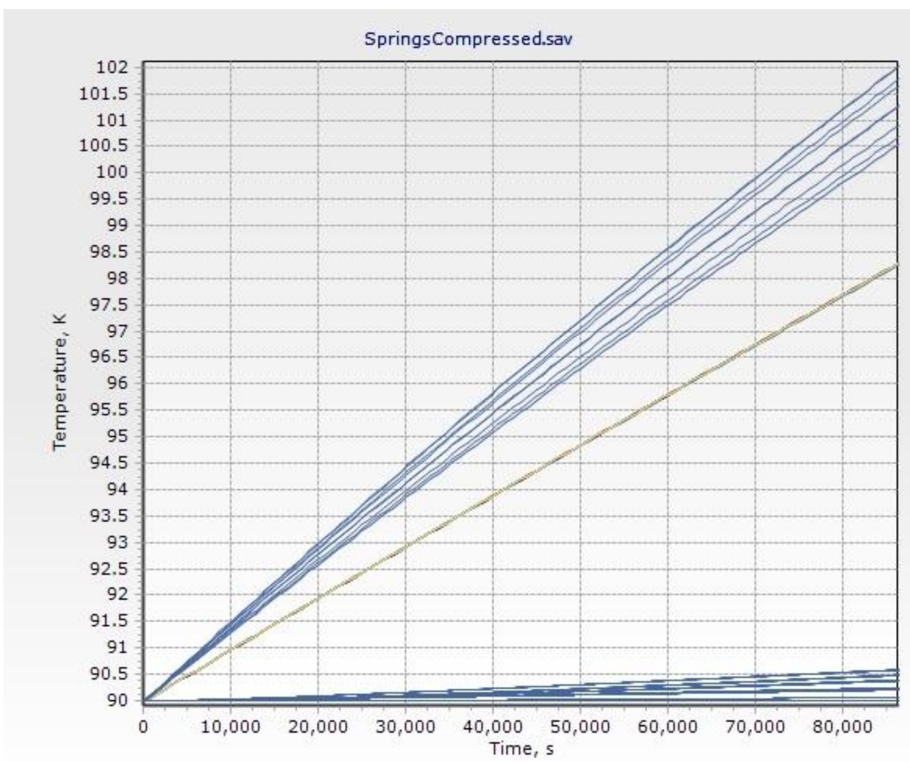
SpringsCompressed.sav
Temperature, K
102
101.5
101
100.5
100
99.5
99
98.5
98
97.5
97
96.5
96
95.5
95
94.5
94
93.5
93
92.5
92
91.5
91
90.5
90
0
10,000
20,000
30,000
40,000
50,000
60,000
70,000
80,000
Time, s

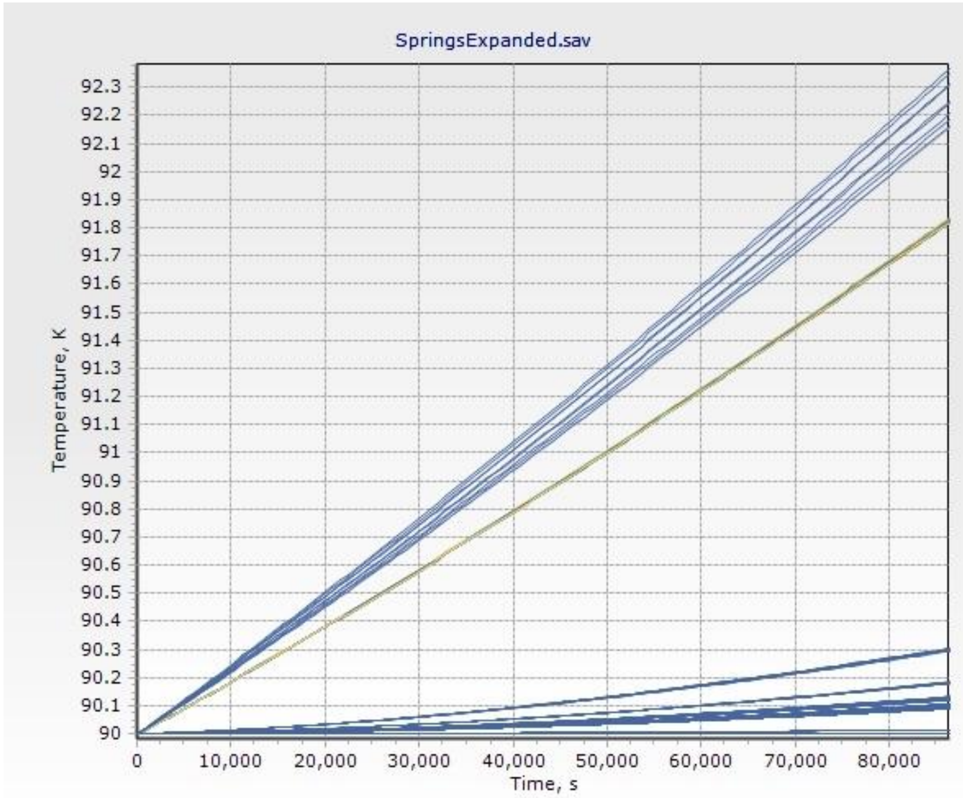
SpringsExpanded.sav
Temperature, K
92.3
92.2
92.1
92
91.9
91.8
91.7
91.6
91.5
91.4
91.3
91.2
91.1
91
90.9
90.8
90.7
90.6
90.5
90.4
90.3
90.2
90.1
90
0
10,000
20,000
30,000
40,000
50,000
60,000
70,000
80,000
Time, s